ARTICLE

Charles W. Wolgemuth · Alexander Mogilner
George Oster

The hydration dynamics of polyelectrolyte gels with applications to cell motility and drug delivery

Abstract We combine the physics of gels with the hydrodynamics of two-phase fluids to construct a set of equations that describe the hydration dynamics of polyelectrolyte gels. We use the model to address three problems. First, we express the effective diffusion constants for neutral and charged spherically distributed gels in terms of microscopic parameters. Second, we use the model to describe the locomotion of nematode sperm cells. Finally, we describe the swelling dynamics of polyelectrolyte gels used for drug release.

Keywords Diffusion constants · Drug release · Hydration dynamics · Nematode sperm cells · Polyelectrolyte gels

Introduction

Gelatinous materials are ubiquitous in nature, from the cell walls of bacteria (Burge et al. 1977) to the human eye (Elliott and Hodson 1998). They find practical applications in fields as diverse as micromachines and drug delivery (Cornejo-Bravo et al. 1995; Siegel et al. 1988). The theory of gel swelling has a long history, beginning with the early work of Flory and Katchalsky (Flory 1953; Katchalsky and Michaeli 1955). More recently, Tanaka and colleagues have addressed the mechanical aspects of gel swelling by treating a neutral gel as a linear elastic solid immersed in a viscous fluid (Tanaka and Fillmore 1979; Tanaka et al. 1973). Although they neglected the motion of the fluid solvent, the model reasonably explained swelling of a gel to a nearby equilibrium volume fraction. Subsequent studies relaxed the constraint of linear elasticity by appealing to a free energy for the polymer mesh and defining the divergence of the stress as the functional derivative of this energy (Durning and Morman 1993; Maskawa et al. 1999; Onuki 1989; Sekimoto et al. 1989; Yamaue et al. 2000). Most of these works still neglected the fluid flow that must accompany swelling. Wang et al. (1997) added in fluid flow by application of two-phase flow theory; however, they considered only the regime of small polymer volume fractions and small gradients in the volume fraction. Durning and Morman (1993) also used continuity equations to describe the flow of solvent and solution in the gel, but used a diffusion approximation with a constant diffusion coefficient to obtain the fluid motion. This assumption does not treat the dynamics of the fluid and the gel on an equal footing, and so it only roughly approximates the viscous drag coupling between the fluid and the polymer. They also proposed a free energy picture that did not include charged gels. Finally, there is a sizeable literature treating the swelling of polyelectrolyte gels in the context of cartilage mechanics. Several authors have used multiphasic fluid models in this setting that include osmotic effects (Gu et al. 1998; Lai et al. 1991; Lanir 1996). Lanir (1996) derived a constitutive relation for polyelectrolyte gels; however, he did not treat the dynamics of the gel. Lai et al. (1991) derived dynamic equations similar to those we derive here using a triphasic theory that also accounts for the flow of salt ions. This treatment, though rigorous in its derivation of the dynamic equations, treats the free energy as a phenomenological function and derives a stress that is only valid for small deformations. Moreover, the energy is treated as a function of strain rather than a functional of position.

In this paper, we draw on the work cited above to unite gel mechanics with two-phase fluid dynamics. The

C. W. Wolgemuth · G. Oster (✉)
Departments of Molecular & Cellular Biology and ESPM,
University of California, Berkeley, CA 94720-3112, USA
E-mail: goster@nature.berkeley.edu
Fax: +1-510-6427428

A. Mogilner
Department of Mathematics and Center for Genetics and Development, University of California, Davis, CA 95616, USA

Present address: C. W. Wolgemuth
Department of Physiology, University of Connecticut Health Center, Farmington, CT 06030, USA

resulting model provides a dynamic description of gel hydration that is suitable for addressing several situations of biological interest. We derive the hydration dynamics of a polyelectrolyte gel immersed in a counterion fluid by combining a Flory-type free energy functional with two-phase fluid dynamics. This model enables us to compute the stresses that act within the gel and to describe the motion of the gel and of the solvent. We apply this model to provide a novel description for the crawling of nematode sperm, and to describe the swelling dynamics of medically important gels from the dry state to equilibrium. Most of the conservation and constitutive equations of the model have appeared in the literature before; however, our derivation of the model is simpler than others, and is more suitable for the biological applications we address.

Methods

A model for polyelectrolyte gels

A polyelectrolyte gel is a charged, cross-linked polymer network immersed in a fluid. Let ϕ denote the volume fraction of the polymer, so that in a unit volume of the gel a fraction of the space, ϕ, is occupied by the polymer and the remaining space is fluid, $(1-\phi)$. The total density of a unit volume of the system is $\rho = \phi\rho_p + (1-\phi)\rho_f$, with ρ_p and ρ_f the density of the polymer and the fluid, respectively. The positions of material points of the polymer are given by the vector X, and we define the initial position of those points at time $t=0$ by x_{init}. The vector $u = X - x_{init}$ defines the displacement of polymer subunits from the initial position. Each of the components obeys a continuity equation:

$$\begin{aligned} \frac{\partial(\phi\rho_p)}{\partial t} &= -\nabla_X \cdot (\phi\rho_p u_t) \\ \frac{\partial((1-\phi)\rho_f)}{\partial t} &= -\nabla_X \cdot ((1-\phi)\rho_f v) \end{aligned} \qquad (1)$$

where $u_t \equiv \partial u/\partial t$ is the polymer velocity, v is the fluid velocity, and ∇_X is the gradient operator with respect to the positions X. Using Eq. (1), and assuming that the fluid and polymer are incompressible (ρ_f = constant, ρ_p = constant), gives the conservation equation:

$$\nabla_X \cdot (\phi 2u_t + (1-\phi)2v) = 0 \qquad (2)$$

As the polymer moves, the polymer volume fraction will change from its initial value, $\phi_{init} \equiv \phi(t=0)$. The following geometrical relationship between ϕ, ϕ_{init}, and u is derived in Appendix A:

$$\frac{\phi}{\phi_{init}} = \det\left(\hat{I} + \frac{\partial u}{\partial x_{init}}\right) \qquad (3)$$

where $\hat{I}$ is the identity matrix. In this paper, we define the *swelling ratio* as the ratio of the initial polymer volume fraction to its final value: ϕ_{init}/ϕ. Equations (2) and (3) describe the kinematics of the two-phase polymer–fluid system.

We shall treat only situations where the Reynolds number is very low, so that the inertia of the polymer and the fluid are negligible compared to the drag forces between them. Therefore, to describe the motion of the gel, we construct a force balance on each phase, with the constraint that the viscous drag between the solid and fluid phases are equal and opposite. For the fluid phase we write a Stokes-like equation (Happel and Brenner 1986):

$$\underbrace{\zeta(v - u_t)}_{\substack{\text{Drag force between}\\\text{fluid and gel}}} = \underbrace{\eta\nabla_X \cdot \left(\frac{\nabla_X v + \nabla_X v^T}{2}\right)}_{\text{Fluid shear stress}} - \underbrace{\nabla_X p}_{\substack{\text{Fluid}\\\text{pressure gradient}}} \qquad (4)$$

Here ζ is the drag coefficient between the polymer and the fluid, η is the fluid viscosity, and p is the fluid pressure. This equation expresses the balance between the force per unit volume acting on the fluid component and the drag force per unit volume that acts between the fluid and polymer. The first term on the right side is the fluid shear, and the second term is the hydrostatic pressure, which we will later relate to the gel osmotic pressure. When the fluid shear term is negligible, it is equivalent to Darcy's law.

We model the polymer mesh as a deformable elastic substance and write its equation of motion as a balance between the viscous drag force and elastic force:

$$\zeta(2u_t - 2v) = 2f^p \qquad (5)$$

where ζ is the same drag coefficient as in Eq. (4), and f^p is the force per unit total volume that acts on the polymer. Adding Eqs. (4) and (5), we find that:

$$\nabla_x \cdot \sigma^T = \nabla_x \cdot \sigma^p - \nabla_x p + \eta\nabla_x \cdot \left(\frac{\nabla_x v + \nabla_x v^T}{2}\right) = 0 \qquad (6)$$

where $\sigma^T = \sigma^p - p\hat{I} + \eta(\nabla_x 2v + \nabla_x 2v^T)/2$ is the total stress and we have used that the force per unit volume that acts on the polymer is related to the polymer stress, σ^p, by $2f^p = \nabla \cdot \sigma^p$. Equations (4) and (5) are coupled because the hydrostatic pressure that acts on the fluid is a function of the stress on the polymer. The coupling is dictated by the volume conservation equation. To complete the equations of motion we require an expression for the force per unit volume acting on the polymer, f^p.

In the literature, the polymer force per volume has been defined either as the divergence of a polymer stress, or the functional derivative of the free energy with respect to position (Onuki 1989). We shall follow the latter strategy:

$$2f^p = \nabla_x \cdot \sigma^p = -\frac{\phi}{\phi_{init}}\frac{\delta F}{\delta X} \qquad (7)$$

where σ^p is the polymer stress tensor, F is the free energy, and $\delta/\delta X$ is the functional derivative with respect to X. The free energy of the gel is the sum of four effects: the gel swells due to (1) the entropic diffusion of its constituent chains and (2) their counterions; swelling is countered by (3) the elastic forces in the chains and (4) interchain attractive forces:

$$F = \underbrace{F_{mix} + F_{ion}}_{\text{Expansion}} + \underbrace{F_{el} + F_{int}}_{\text{Contraction}} \qquad (8)$$

Figure 1 illustrates these effects in a cartoon. In this model, we do not directly account for the electrostatic repulsion of fixed charges on the polymer; however, when the ion diffusion is fast compared to the dynamics of the polymer and the bath ionic strength is low, the electrostatic effects do not contribute to the total free energy (see Appendices B and C). In Appendix B we give explicit expressions for each of these terms. The expression for σ^p that results from taking the functional derivative of Eq. (8) is derived in Appendices B and C. [These model equations are similar to those derived for two-phase fluid flow without elastic forces derived by He and Dembo (1997) and also the triphasic theory developed by Lai et al. (1991).] The model gel is described by Eqs. (1, 2, 3, 4, 5, 6, 7, 8) with appropriate boundary conditions. The model variables are listed in Table 1.

Results

Applications of the model

Diffusive swelling of gels

One of the earliest dynamic models for a gel was formulated by Tanaka and colleagues (Tanaka et al. 1973).

Swelling Pressure
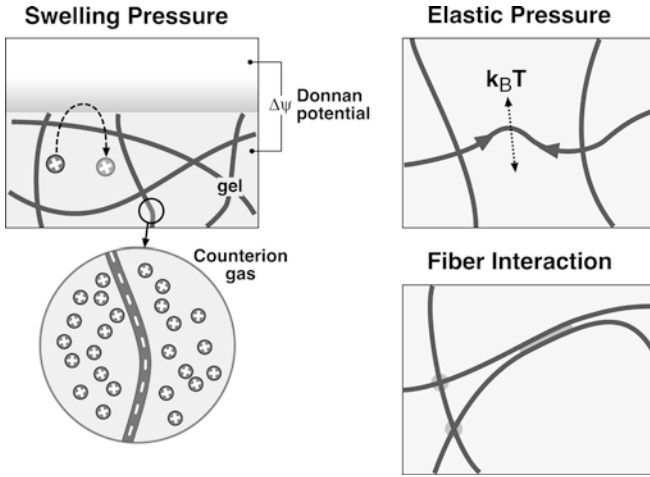
Elastic Pressure

Fiber Interaction

Fig. 1 Cartoon illustration of the terms in the free energy expression (Eq. 1). The counterion swelling pressure (*left panel*) arises from the diffusion of the mobile counterions (+) to the fixed fiber charges (−) that give rise to the Donnan potential at the gel surface. The contractile elastic pressure (*right top*) arises from the transverse thermal fluctuations of the gel fibers that tend to pull the crosslinks together. The fiber interaction (r*ight bottom*), which may be electrostatic or hydrophobic, also tends to deswell the gel by reducing the chain entropy

Table 1 Model variables

Symbol	Definition	Units
ϕ	Volume fraction of gel	Dimensionless
$\boldsymbol{u}$	Gel displacement	cm
t	Time	s
$\boldsymbol{v}$	Fluid velocity	cm/s
$\boldsymbol{x}$	Position	cm
p	Hydrostatic pressure	dyn/cm^2
σ	Gel stress	dyn/cm^2
F	Free energy	dyn cm
C_b	Counterion concentration	M
h	Stress due to changes in volume	Dimensionless

They assumed that the fluid remained stationary and that the gel polymer behaved as a linear elastic solid. For the swelling of a spherically symmetric gel, these assumptions led to a diffusion equation with a diffusion coefficient as the ratio of the elastic modulus to the drag coefficient between the fluid and the gel. This model fit well the experiments on the swelling of neutral gels near equilibrium. Since then, a number of dynamic models have been proposed that introduce a nonlinear elastic constitutive relation for the gel polymer or incorporate solvent coupling. All of these have been shown to reduce to a diffusion equation in the limit that the relative change in volume of the gel is small. Likewise, our model also reproduces this result (see Appendix D). This diffusive behavior arises for small changes in the gel volume as the motion of solvent becomes negligible and deformations of the polymer remain in the linear elastic regime. These were the assumptions used to derive the original diffusive model (Tanaka et al. 1973).

However, we can make further progress: since the model utilizes a microscopic constitutive relation with experimentally measurable parameters, the diffusion coefficient for the gel can be estimated as a function of microscopic model parameters. Using the linearized model equations given in Appendices D and E with reasonable values for the gel parameters (see Table 2), we compute the diffusion coefficients for neutral gels with a 5% and 2.5% equilibrium polymer volume fraction: $D_5 = 6.8 \times 10^{-7}$ cm^2/s and $D_{2.5} = 4.6 \times 10^{-7}$ cm^2/s, respectively. These values are comparable to the diffusion constants observed experimentally for gels. For these volume fractions, the ratio $D_5/D_{2.5} = 1.45$ has been experimentally measured for neutral gels (Tanaka et al. 1973). The model also elucidates the dependence of the diffusion constant on the free counterion charge. Figure 2 shows how the swelling rate increases with the effective free ion charge per monomer, α. As the gel polymer becomes more charged, the diffusion constant increases. Qualitatively, this effect is due to the contribution of the counterions to the osmotic pressure at the gel boundary, so that polyelectrolyte gels swell much more rapidly than neutral gels.

Crawling of nematode sperm

Many cell types can glide across a surface while maintaining their overall shape using a motile appendage called a lamellipod (see Fig. 3a) (Bray 2001). The sperm of the nematode *Ascaris suum* has attracted much attention recently because it represents a "stripped down" version of a motile cell (Bottino et al. 2002; Roberts and Stewart 2000). The sperm cell is tens of microns long and wide and a few microns high. It advances steadily at a rate of ~0.1 μm/s. A polymer network permeates the ventral surface consisting of flexible filaments composed of major sperm protein (MSP). The filaments are positively charged, having polymerized from highly basic dimers. Strong hydrophobic interactions between the polymers aggregate them into higher order rope-like complexes. The cell body that contains the nucleus and mitochondria rides atop the cytoskeletal network at the rear of the cell (see Fig. 3). Mitochondrial activity maintains a spatial pH gradient across the lamellipod such that the cytoplasm at the rear is acidic with respect to the front of the cell. There is evidence that the local pH controls motility by affecting cell adhesion, protrusion, and contraction (Bottino et al. 2002).

The strength of adhesion of the lamellipod to the surface increases with decreasing pH. Thus the cell attaches to the surface strongly at the front and weakly towards the rear. At the leading edge of the cell MSP dimers assemble onto the tips of existing polymers, pushing the leading edge forward (Bottino et al. 2002; Mogilner and Oster 1996). The rate of protrusion is indirectly regulated by the pH gradient and decreases with cell length. MSP filaments depolymerize in the low pH environment at the rear of the cell and MSP dimers

Table 2 Model parameters

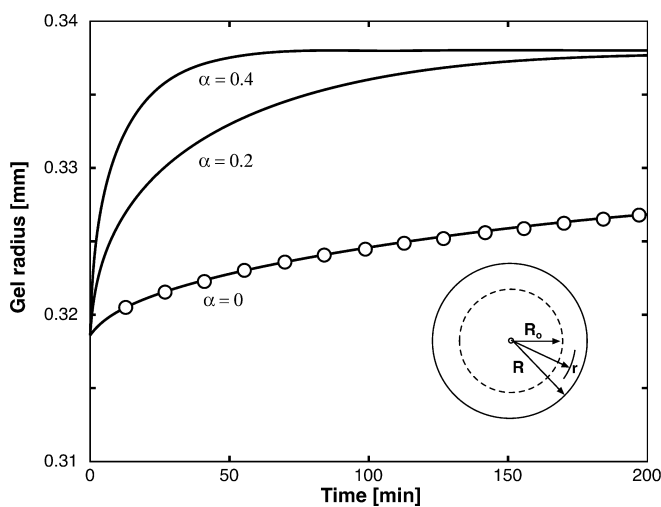| Symbol	Definition	Value and units
ϕ_{init}	Initial polymer volume fraction	0.025, 0.1
ζ	Drag coefficient between the polymer and the fluid	2×10^{11} dyn s/cm^4 (Tanaka and Fillmore 1979)
η	Fluid viscosity	100 dyn s/cm^2
V_m	Volume of a monomer	0.1–1 nm^3 (English et al. 1996)
μ	Gel shear modulus	200 dyn/cm^2 (Tanaka and Fillmore 1979)
ϕ_0	Material parameter setting unstressed volume fraction	$\sim$0.1
$k_B T$	Thermal energy	$\sim$4.1 pN nm
N_A	Avogadro's number	6.02×10^{23}
N_x	Number of monomers between crosslinks	$\sim$10–100 (English et al. 1996)
χ	Flory interaction parameter	0.6 (English et al. 1996)
D	Diffusion coefficient of the gel	$\sim$10^{-7} cm^2/s (computed here)
α	Number of charges per monomer	$\sim$0.05 (assumed)
C_b	Bath ion concentration	$\sim$0.07 M (assumed)
κ	Permeability of gel/solvent interface	$\sim$10^{-9} cm^3/dyn s

Fig. 2 Model prediction of the swelling of a polyelectrolyte gel compared to a neutral gel. α is the effective number of counterions per gel monomer. The *circles* are data points from Tanaka et al. (1973). The *curves* for $\alpha = 0.2$ and 0.4 were computed from the linearized model equations given in Appendices D and E

Fig. 3 **a** Side view of a crawling nematode sperm showing the gel strip model. (**b**) Asymptotically stable stationary distributions of the polymer volume fraction, stress, and velocity and of the fluid velocity from the rear to the front of the cell. (**c**) Trajectories of the front and rear ends of the 1-D cytogel strip. Over a few hundred seconds the cell length regulates to a constant value

are recycled from the rear to the front by simple diffusion. The model of Bottino et al. (2002) is based on the assumption that at high pH the MSP polymers aggregate into bundles storing elastic energy and generating the force of protrusion. Then, in the low pH environment under the cell body, the adhesions between the filaments weaken and the complexes dissociate. This releases the elastic energy stored in the gel so that it can entropically contract and pull the rear of the cell forward.

Bottino et al. (2002) developed a 2-D finite element model of the moving sperm cell, where the MSP gel was treated as elastic solid and the fluid part of the cytoplasm was neglected. Here we consider the sperm cell cytoskeleton as a hydrated polyelectrolyte gel governed by the equations derived in this paper. This allows us to advance the model of cell crawling by explicitly taking into account the mo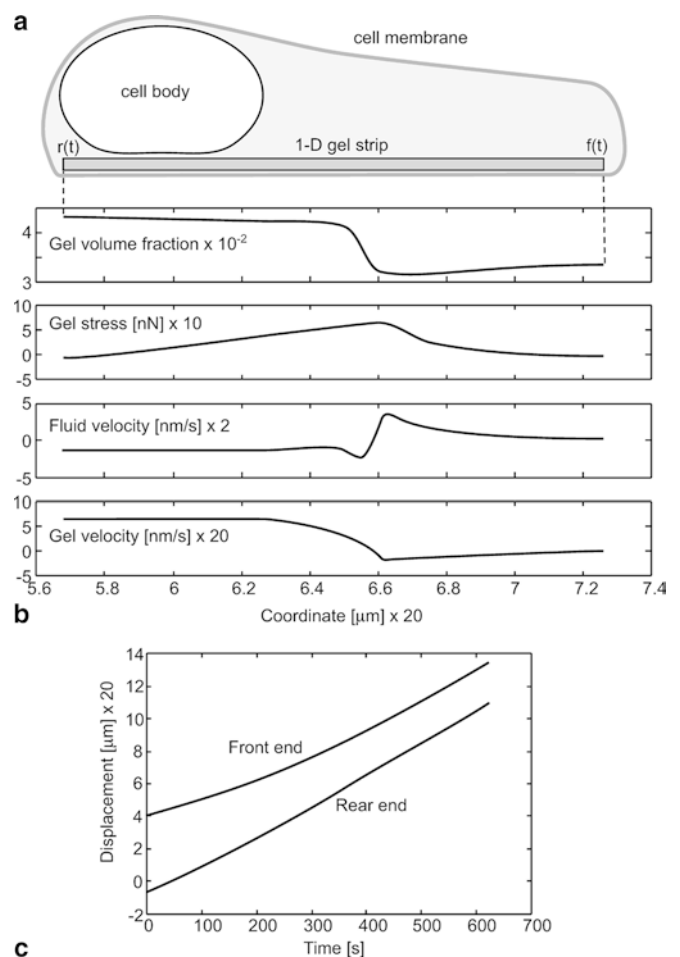vement of the liquid fraction of the cytoplasm and including the effects of ion osmotic pressure. This allows us to compute the forces of the gel contraction microscopically, rather than relying on a

phenomenological contractile stress constitutive relation. Following Bottino et al. (2002), this model assumes rubber-like elasticity for the MSP polymer: individual filaments appear to be fairly flexible; there are no direct measure of their persistence length but negatively stained filaments are curved and bent on the scale of tens of nanometers. We neglect chemical reactions in our equations of mass balance because of the very high (~4 nM) concentration of MSP in the cytoplasm (Roberts and Stewart 2000). There are experimental indications (Bottino et al. 2002; Roberts and Stewart 2000) that a small number of enzymes activate MSP dimers into a polymerizable state, and that this is the rate-limiting factor for MSP fiber assembly. Also, diffusion of MSP dimers is fast enough to recycle the dimers from the rear to the front of the cell. Because of these factors, equations of chemical kinetics and diffusion uncouple from the equations for MSP gel, and our model for the gel is self-consistent. The situation is more complicated for actin gels, and future work will incorporate semi-flexible polymer energies and reaction-diffusion kinetics into the gel dynamic model to explore the quantitative differences between rubber-like and semi-flexible polymers and the role of MSP turnover. Here we report the results of a 1-D simulation of a proximal-distal transect of the cytoskeletal gel strip at the center of the lamellipod. A 2-D simulation that takes into account processes at the cell sides is much more involved numerically; this work is in progress and will be reported elsewhere; however, the 1-D model illustrates all of the basic features driving the cell locomotion.

We model the dynamics of the 1-D cytoskeletal strip of gel solving the model equations (Eqs. 1, 2, 3, 4, 5, 6, 7) on a moving boundary domain. The quantitative details are presented in Appendix H. The rates of movement of the cell leading and trailing boundaries are given by the boundary velocities plus the rate of polymerization at the front and depolymerization at the rear, respectively. We assume that the depolymerization rate is constant. We make the following assumptions consequent on the proximal to distal pH gradient. (1) The polymerization (protrusion) rate at the front is a decreasing function of the cell length. (2) There is an effective viscous drag between the cytoskeleton and the substratum; the corresponding viscous drag coefficient increases significantly anterior to the cell body. (3) We model the unbundling of MSP filaments at the rear by increasing the number of MSP dimers between adjacent crosslinks under the cell body. We complement the model equations by the conditions of zero gel stress at the boundaries and no fluid flow through the leading edge boundary. This amounts to assuming that the major fluid flow into the basal gel strip comes from the cytoplasm "above" the ventral layer we are modeling. From the viewpoint of the 1-D model this enters as a distributed fluid source.

Figure 3c shows the trajectories of the leading and trailing edges of the cell. After initial transients decay, the steady mode of locomotion evolves such that the cell achieves a constant length of tens of microns, similar to the observed length. It advances at the rate of few tenths of micron per second, in agreement with experimental observations (Roberts and Stewart 2000). In the coordinate system moving with the cell, constant spatial distributions of densities, velocities, and forces inside the cell also evolve. Figure 3b shows asymptotically stable spatial distributions of the polymer volume fraction, stress, gel and liquid velocities. The highly crosslinked, unstressed gel has a steady-state polymer volume fraction ~0.03. At the rear of the lamellipod, just in front of the cell body, the number of crosslinks drops precipitously. Longer flexible polymer chains between the adjacent crosslinks have a tendency to coil, like rubber strands (see Appendix H), so that the polymer volume fraction, ϕ_0, increases. External and internal viscous drag retards the polymer volume increase. Thus a contractile gel stress develops that reaches its maximum at the center of the cell. The predicted total contractile force is tens of nanonewtons, comparable to that estimated experimentally for some other crawling cells (Oliver et al. 1995). This contractile stress does not affect the front of the cell because the adhesion to the substratum is strong at the front. However, because the adhesion is weak at the rear, this contractile stress pulls the rear of the cell forward. The contractile stress tends to compress the gel at the rear of the cell, where the polymer volume fraction reaches a new steady value of ~0.045, relieving stress at the rear.

The rate of advancement of the leading edge is equal to the polymerization rate. The steady state velocity of ~0.1 μm/s at the cell rear is a consequence of the gel contraction velocity that just balances the constant polymerization rate at the front. The balance of forces is such that if the lamellipod increases in length the protrusion velocity decreases, while at smaller length it increases, so the cell length is stable. The boundary condition at the front ensures that the fluid velocity is zero there. However, in the middle of the cell, the large contractile stress creates a significant hydrostatic pressure which drives the fluid phase of the cytoplasm both forwards and backwards. At the very rear of the cell, the water escapes upward into the region of the cell around the cell body, where the cytoskeletal gel is less dense. Consequently, the cytoplasm near the dorsal surface of the cell should convect towards the front where new gel is polymerized. Computations show that the movement of the fluid is slow (a few nanometers per second) in comparison with gel movements. This justifies the corresponding assumption made by Bottino et al. (2002). Thus, the model illustrates how stable rapid migration is achieved, so that the cell length and velocity regulate to constant values.

Swelling and hydration dynamics in drug delivery

Gel swelling has many applications in the field of drug delivery. One method is to chemically bind the drug to

the gel matrix and release it enzymatically (Tzafriri 2000; Tzafriri et al. 2002). Another method is to trap a drug within the polymer mesh of a dehydrated gel. When the gel is ingested, the gel swells until the mesh spacing is large enough for the drug to diffuse out of the network. In this way, it is possible to control the rate at which the drug is administered. To quantify this effect it is important to understand the dynamics of a gel swelling from a dry state, and there has been a wealth of experiments on the swelling of gels from the dry to equilibrium volume fraction. These curves tend to show a biphasic behavior where the gel initially swells at a fairly constant rate, then goes through a very rapid transition, and finally settles down to its equilibrium configuration (Siegel et al. 1988). This swelling behavior has been attributed to a dry core that inhibits the swelling until the core hydrates, after which the rest of the gel can swell more freely. Previous theoretical work has shown that under certain conditions a sharp moving interface arises between a dry and swollen region (Tomari and Doi 1995). Recent experiments verified the existence of this dry core region during the swelling of a spherical poly(0.75 sodium acrylate–0.25 acrylic acid) gel (Budtova and Navard 1998). Here we show that our model explains quantitatively the hydration dynamics of a swelling gel from the dry state.

We use a dynamic equation for the polymer volume fraction, ϕ, in a Lagrangian frame of reference with respect to the initial coordinates (see Appendix E) and solve the equations for a spherically symmetric volume, whereupon the coupled dynamic equations for the gel reduce to one equation (Eq. E4). To determine whether these equations can model the swelling of a spherical gel from a dry, glassy state to the swollen, rubbery state, we compute the model equations in the two-phase region by adjusting the Flory interaction parameter so that the free energy of the gel is bistable (i.e., it possess two minima). The first of these minima represents the glassy state at high volume fractions where polymers tend to associate and align. The other minimum represents the swollen state of the gel. At high volume fractions, polymer attraction drives the formation of the glassy state; we model this behavior by making the polymer–polymer interaction a function of the volume fraction (see Appendix B). Following the experimental conditions, we solve Eq. (E4) for the swelling of an initially dry sphere, using a drag coefficient between the fluid and solid components that depends on the polymer volume fraction (see Appendix G and Budtova and Navard 1998). As in the experiments, we plot both the normalized radius of the sphere, $R(t)/R_{max}$, and the normalized radius of the dry core versus time, where R_{max} is the final swollen radius of the sphere. The solution shown in Fig. 4 is consistent with the suggestion of Siegel that the presence of the glassy core puts a constraint on the swelling of the rubbery periphery (Siegel et al. 1988). Once the swelling front reaches the center of the gel, the glassy core disappears
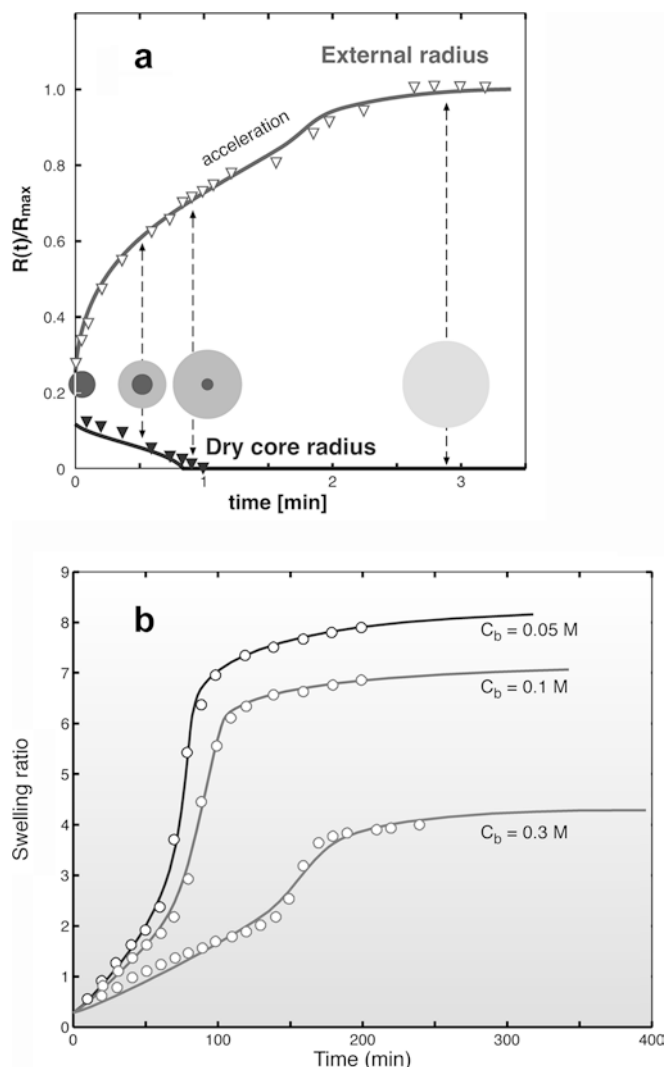

Fig. 4 The swelling of an initially dry polyelectrolyte sphere to its equilibrium volume. Data points (*open and closed triangles*) are taken from Budtova and Navard (1998, Fig. 2). The *top curve* shows the time course of the external radius of the gel. The *lower curve* corresponds to the radius of the interface between the dry core and the swollen phase. The *insets* illustrate the swelling of the sphere and the disappearance of the dry core. The acceleration in the swelling that occurs once the dry core vanishes is labeled

and the swelling is unconstrained. At this point, a sudden acceleration is observed when the glassy core disappears (see Fig. 4). After this transient acceleration, the swelling slows and the radius approaches its equilibrium value. A more complete physical description of this process will be presented elsewhere (Burfoot and Wolgemuth, unpublished).

Since we can fit the observed swelling behavior by our model, this suggests that optimization techniques could be applied to "program" release rates from gels with simple geometries, e.g. spheres, cylinders, and disks. The experimental data from the dynamics of swelling also allows us to predict the microscopic parameters that are used in our model (see Appendix G).

Conclusion

We have assembled a model for the dynamics of poly-electrolyte gels from previously published components that treat the gel as an elastic solid immersed in fluid. We describe the dynamics by conservation equations for polymer and fluid complemented by Stokes-like stress balance equations for the polymer and fluid. The principal novelty of the model is that it combines two-phase fluid flow, functional derivatives and a free energy derived from Flory theory that contains microscopically measurable parameters. Though none of these separate concepts is new, this model fully integrates them into a fairly simple theory, generating predictions that can be tested against experimental data.

The model allows us to derive an effective diffusion equation for the swelling of neutral and charged gels that generalizes previous work, and accounts for the fluid movements that accompany gel swelling and de-swelling, factors that have been largely neglected heretofore. This enables us to express the effective diffusion coefficient of the gel in terms of microscopic, rather than phenomeno-logical macroscopic, parameters, revealing how swelling accelerates as the gel charge increases. The main novel application of the model is the quantitative description of the lamellipodia of the nematode sperm cell. The model explains the nature of contractile stress that, when coupled to graded adhesion and depolymerization, drives the cell forward. The model reproduces some important features of steady cell movement. Finally, we model the isotropic swelling of charged gels. Solving the model in the two-phase region accounts for the glassy state of the dry gel. The model captures the qualitative features of the experimental data on the swelling of spherical gels employed for controlled drug release, and explains the observed biphasic swelling dynamics. This theory describes semi-quantitatively the swelling of a gel from the dry state all the way to equilibrium.

Future elaborations of the model can deal with specific geometries where shear stresses are important and swelling is driven or accompanied by chemical kinetics. This should be useful in a number of fields, including biomedical applications and cell mechanics.

Appendix

Appendix A: elasticity and functional derivatives

To define the stress tensor for the polymer mesh, Tanaka et al. (1973) originally assumed that the gel could be treated as an elastic solid with an elastic energy given by:

$$F_{el} = \int \left[\mu \left(u_{ik} - \frac{1}{3} u_{jj} \delta_{ik} \right)^2 + \frac{1}{2} K u_{jj}^2 \right] d^3 x \quad (A1)$$

Here the components of the strain tensor are $u_{ik} = (\partial u_i / \partial X_k + \partial u_k / \partial X_i)/2$, μ is the shear modulus, and K is the bulk modulus. The first term in the integral is the energy associated with shear deformations of the solid and the second term is the energy associated with changes in volume. Moreover, they assumed that the solvent was stationary and set the viscous drag force acting on the gel polymer equal to the force obtained from the functional derivative of this energy (Tanaka et al. 1973). Here we introduce a more complete description of the free energy of the polyelectrolyte gel by taking into account not only the elastic energy but the mixing, counterion, and polymer interaction energies as well (English et al. 1996).

The energy we will use is dependent on two parameters, the metric determinant, $\sqrt{g} = \frac{\phi_{init}}{\phi}$, and the trace of the metric, $\text{Tr}(g_{ij}) = \frac{\partial X_i}{\partial x_j} \frac{\partial X_i}{\partial x_j}$. As such, the energetic cost for deformations of the gel can be written as:

$$F = \iiint_V \left(\Theta(\phi) + \frac{\phi}{\phi_{init}} \Upsilon(\text{Tr}(g_{ij})) \right) d^3 X \quad (A2)$$

with Θ and Υ functions that describe the energetic cost for volume and volume/shear deformations, respectively, and the integral being taken over the volume of the gel, V. This appendix defines notation and shows how functional derivatives are calculated and used to derive the forces per volume that act on the polymer mesh.

We begin by defining the position of points in the polymer mesh through the vector X. The initial position of the polymer mesh at time $t = 0$ is $x_{init} = x(t = 0)$. From this, we can define the displacement vector for these material points as $u = X - x_{init}$. The volume fraction of the polymer is obtained from this by:

$$\frac{\phi_{init}}{\phi} = det\left[\frac{\partial X}{\partial x_{init}} \right] = det\left[\hat{I} + \frac{\partial u}{\partial x_{init}} \right] = \sqrt{g} \quad (A3)$$

with ϕ_{init} the initial polymer volume fraction and $\hat{I}$ the identity matrix. Using this notation, we now discuss how to derive the force from a given energy function. To better elucidate the method, we begin by considering only deformations that change the volume. The variation in the energy is taken with respect to the initial position vector, x_{init}, over the initial volume, V_0, as the limits of this integration are not altered by the variation:

$$\delta F = \iiint_{V_0} \frac{\partial}{\partial \phi} \left[\frac{\phi_{init}}{\phi} \Theta(\phi) \right] \delta\phi d^3 x_{init} \quad (A4)$$

It can be shown (Onuki 1989) that:

$$\delta\phi = -\phi \sum_{l,m} \left[\frac{\partial x_{\text{init},m}}{\partial X_l}\right]\left[\frac{\partial}{\partial x_{\text{init},m}}\delta X_l\right] = -\phi\sum_l\left[\frac{\partial}{\partial X_l}\delta X_l\right]$$

$$\text{(A5)}$$

Substituting this expression into Eq. (A4) and transforming back to the displaced coordinates, we obtain:

$$\delta F = \iiint_V \left(-\frac{\phi^2}{\phi_{\text{init}}}\right)\frac{\partial}{\partial\phi}\left[\frac{\phi_{\text{init}}}{\phi}\Theta(\phi)\right]\sum_l\left[\frac{\partial}{\partial X_l}\delta X_l\right]\mathrm{d}^3X$$

$$\text{(A6)}$$

This is then integrated by parts to give:

$$\delta F = -\iint_{\partial V}\sum_{l,m}n_m\Pi^{\mathrm{p}}_{lm}\delta X_l\,\mathrm{d}A +_V\sum_{l,m}\left[\frac{\partial}{\partial X_m}\Pi^{\mathrm{p}}_{lm}\right]\delta X_l\,\mathrm{d}^3X$$

$$\text{(A7)}$$

where $\boldsymbol{n}$ is the unit outward normal vector to the surface element $\mathrm{d}A$, ∂V is the surface of the gel, and the isotropic polymer stress due to changes in volume is defined as:

$$\Pi^{\mathrm{p}}_{lm} = \left(\phi\frac{\partial\Theta}{\partial\phi} - \Theta\right)\delta_{lm}$$

$$\text{(A8)}$$

This also gives a force per volume:

$$2f^{\mathrm{p}} = -\nabla_X\cdot\Pi^{\mathrm{p}}$$

$$\text{(A9)}$$

where ∇_X is the gradient over the displaced coordinates, $\boldsymbol{X}$.

In a similar fashion, we can find the stress from the trace term:

$$\sigma_{\text{tr},ij} = -\frac{\phi}{N_x V_m}\sum_l\frac{\partial X_i}{\partial x_l}\frac{\partial X_j}{\partial x_l}$$

$$\text{(A10)}$$

and we have used that:

$$\Upsilon = \frac{\phi_{\text{init}}}{N_x V_m}\text{Tr}(g_{ij})$$

$$\text{(A11)}$$

Combining these two terms, the total stress on the polymer is:

$$\sigma^{\mathrm{p}}_{ij} = \Pi^{\mathrm{p}}_{ij} + \sigma_{\text{sh},ij}$$

$$\text{(A12)}$$

Appendix B: components of the gel free energy

The total free energy for the gel component can be broken up into six independent components arising from the elasticity of the polymer, the entropic mixing due to the fluid, interactions between polymer chains, the pressure due to the counter ions, Coulombic interactions, and a term that depends on gradients in the volume fraction as:

$$F = F_{\text{el}} + F_{\text{mix}} + F_{int} + F_{\text{ion}} + F_{\text{coulomb}} + F_{\text{grad}}$$

$$\text{(B1)}$$

We choose an elastic free energy based on rubber elasticity (Flory 1953):

$$F_{\text{el}} = \frac{k_B T}{2N_x V_m}\iiint_V \phi\left[\text{Tr}(g_{ij}) - 3 - ln\left(\frac{\phi_0}{\phi}\right)\right]\mathrm{d}^3X$$

$$\text{(B2)}$$

where ϕ is the polymer volume fraction, g_{ij} is the metric between the initial coordinates, $\boldsymbol{x}$, and the final coordinates, $\boldsymbol{X}$, k_B is Boltzmann's constant, T the absolute temperature, N_x the number of monomers between crosslinks, ϕ_0 is a material parameter that sets the unstressed volume fraction, V_m is the equivalent volume occupied by one monomer, and V is the volume of the gel. From these definitions, the number of chains per volume is $\phi/N_x V_m$. For the isotropic case:

$$g_{ij} = \left(\frac{\phi_{\text{init}}}{\phi}\right)^{2/3}\hat{I}$$

$$\text{(B3)}$$

and:

$$F_{\text{el}} = \frac{k_B T}{2N_x V_m}\iiint_V \phi\left[\left(\frac{\phi_0}{\phi}\right) - 1 - \frac{1}{3}ln\left(\frac{\phi_0}{\phi}\right)\right]\mathrm{d}^3X$$

$$\text{(B4)}$$

We choose the entropic mixing free energy defined by Flory theory (Flory 1953):

$$F_{\text{mix}} = \frac{k_B T}{V_m}\iiint_V (1 - \phi)ln(1 - \phi)\mathrm{d}^3X$$

$$\text{(B5)}$$

and the solvent–polymer interaction energy representing two-body interactions is given by:

$$F_{int} = \frac{k_B T}{V_m}\iiint_V \chi\phi(1 - \phi)\mathrm{d}^3X$$

$$\text{(B6)}$$

where χ is the Flory parameter that measures the strength of interaction between the polymer chains (Flory 1953). It is common to assume that χ is independent of volume. However, in principle, it can be a function of ϕ; here we assume a dependence:

$$\chi = \chi_0 + \chi_1\phi^2$$

$$\text{(B7)}$$

to approximate the glass–rubber transition for swelling gels.

The contribution to the energy from the counterions is obtained by assuming an ideal solution of charges with each species of charge labeled by the subscript i (English et al. 1996):

$$F_{\text{ion}} = -k_B T N_A \iiint_V \sum_i C_i ln(C_i)(1 - \phi)\,\mathrm{d}^3X$$

$$\text{(B8)}$$

where C_i is the molar concentration of the ith mobile counterion and N_A is Avogadro's number. The factor of $(1-\phi)$ in the integral is because the ions only reside in the fluid component of the mixture. Likewise, C_i is the concentration with respect to the fluid volume, $\mathrm{d}V^f$, not the total volume, $\mathrm{d}V^T$.

The contribution to the free energy from Coulombic interactions is:

$$F_{\text{coulomb}} = \iiint_V \sum_i z_i e \Phi_{\text{self}} C_i \, d^3X + \iiint_V z_{\text{F}} e \Phi_{\text{self}} C_{\text{F}} \, d^3X \tag{B9}$$

where z_i is the valence of the ith mobile counterion, e is the electronic charge, ϕ_{self} is the self-consistent potential created by the polymer charges and the mobile ions, and C_{F} is the fixed charge density of the polymer.

For cases where large differences in the volume fraction might exist over small lengths, such as volume-phase transitions in gels (Sekimoto et al. 1989; Tanaka 1997), it is common to include a term that defines the energy required to maintain the sharp gradient. As in Landau–Ginzburg theory and Cahn–Hilliard theory (Cahn and Hilliard 1958), we assume the form of the energy to be:

$$F_{\text{grad}} = \iiint_V \frac{\gamma}{2} \nabla \phi \nabla \phi \, d^3X \tag{B10}$$

where γ is a material parameter that has units of energy/length. This type of energy has already been suggested for gels (Tanaka 1997).

Appendix C: the counterion swelling pressure of the gel

In Eq. (B8), the energy of the counterions is that of an ideal solution of charges. We assume that the diffusion of the ions is much quicker than the motions of the solvent and polymer. Therefore, we use the steady-state concentrations for the ions inside the gel. Because the counterions are confined within the solvent, the concentration is taken with respect to the solvent volume, $dV^{\!f} = (1-\phi)dV^{\text{T}}$, where dV^{T} is a total unit volume of the gel. If we assume that there is an effective charge per monomer, α, on the polymer, the fixed charge density of the polymer is equal to $\alpha N/(dV^{\!f})$ where $N = \phi/V_{\text{m}}$ is the number of monomers per volume and V_{m} is the volume of a monomer. From this, the fixed charge density of the polymer is:

$$C_{\text{F}} = \frac{\alpha \phi}{(1-\phi)V_{\text{m}}} \tag{C1}$$

Assuming a univalent salt in the solvent, the concentrations of the positive and negative ions, C_+ and C_-, respectively, can be related to the fixed charge density via the Donnan equilibrium (Overbeek 1956). Equating the chemical potentials across the boundary:

$$\begin{aligned} C_+ &= \frac{1}{2}\left(\left(4C_{\text{b}}^2 + C_{\text{F}}^2\right)^{1/2} - C_{\text{F}} \right) \\ C_- &= \frac{1}{2}\left(\left(4C_{\text{b}}^2 + C_{\text{F}}^2\right)^{1/2} + C_{\text{F}} \right) \end{aligned} \tag{C2}$$

where C_{b} is the bulk molar concentration of positive (or negative) ions outside the gel. Therefore, the total molar ion concentration inside the gel, $C_{\text{ion}} = C_+ + C_-$, can be related to the fixed charge concentration:

$$C_{\text{ion}} = 2C_{\text{b}}\sqrt{1 + \left(\frac{\alpha\phi}{2(1-\phi)N_{\text{A}}V_{\text{m}}C_{\text{b}}}\right)^2} \tag{C3}$$

Note that in the limit of the neutral gel, $C_{\text{ion}} = 2C_{\text{b}}$ ($2C_{\text{b}}$ is the total ion bath concentration), while in the limit of a highly charged gel, the concentration is $(1/V_{\text{m}})(\alpha\phi/(1-\phi))$. As $\phi \to 1$, this concentration diverges. We expect that the effective fixed charge per monomer decreases with volume fraction due to the condensation of charges onto the polymer as the gel dehydrates. Demanding that in the absence of solvent all the charges are condensed onto the polymer sets $\alpha(\phi = 1) = 0$. To satisfy this constraint, we choose $\alpha = \alpha_0(1-\phi)$, with α_0 a constant.

Using Eqs. (C1) and (C2), we can find the Coulombic contribution to the energy:

$$\begin{aligned} F_{\text{coulomb}} &= \iiint_V e\Phi_{\text{self}}(C_+ - C_-) \, d^3X + \iiint_V z_{\text{F}} e\Phi_{\text{self}} C_{\text{F}} \, d^3X \\ &= \iiint_V -e\Phi_{\text{self}} C_{\text{F}} \, d^3X + \iiint_V z_{\text{F}} e\Phi_{\text{self}} C_{\text{F}} \, d^3X \\ &= 0 \end{aligned} \tag{C4}$$

Therefore, the electrostatic contribution to the total free energy is zero. This is only valid at low ionic strengths and when the diffusion of the ions is much quicker than the dynamics of the polymer.

The free energy for the gel can now be written completely in terms of the polymer volume fraction and a shear term. Using the free energy given in Appendix B and Eq. (A8) and (A10) to calculate the polymer stress, we find:

$$\left(\frac{V_{\text{m}}}{k_{\text{B}}T}\right)\Pi_{ij}^{\text{p}} = h(\phi)\delta_{ij} - \frac{\phi}{N_{\text{x}}V_{\text{m}}}\sum_l \frac{\partial X_i}{\partial x_l}\frac{\partial X_j}{\partial x_l} \tag{C5}$$

where:

$$\begin{aligned} h(\phi) = &-\ln(1-\phi) - \phi - \chi\phi^2 + N_{\text{A}}V_{\text{m}}(C_{\text{ion}} - 2C_{\text{b}}) \\ &+ \frac{\phi}{2N_{\text{x}}} + \gamma\left(\phi\nabla^2\phi - \frac{1}{2}(\nabla\phi)^2\right) \end{aligned} \tag{C6}$$

Experiments have shown that, at low volume fractions, the gel shear modulus is much less than the bulk modulus (Tanaka and Fillmore 1979). If we neglect the shear component [which is the same as using the isotropic form of the elastic free energy (Eq. B4)] and the term that comes from the gradient squared piece in the energy, the polymer stress in Eq. (C5) reduces to:

$$\left(\frac{V_{\mathrm{m}}}{k_{\mathrm{B}}T}\right)\Pi_{ij}^{\mathrm{p}} = h(\phi)\delta_{ij} \tag{C7}$$

where:

$$h(\phi) = -ln(1-\phi) - \phi - \chi\phi^2 + N_{\mathrm{A}}V_{\mathrm{m}}(C_{\mathrm{ion}} - 2C_{\mathrm{b}})$$
$$+ \frac{\phi_0}{N_{\mathrm{x}}}\left(\frac{1}{2}\left(\frac{\phi}{\phi_0}\right) - \left(\frac{\phi}{\phi_0}\right)^{\frac{1}{3}}\right) \tag{C8}$$

is the dimensionless swelling pressure and we have assumed that the parameters χ, ϕ_0, α_0, N_{x}, and γ are constants. We have also subtracted $2N_{\mathrm{A}}V_{\mathrm{m}}C_{\mathrm{b}}$ to account for the ion pressure outside the gel.

If we only assume a purely entropic energy as given by Eq. (B5), then:

$$h(\phi) = -ln(1-\phi) - \phi \tag{C9}$$

Plugging this into Eqs. (5) and (7), we find that:

$$\zeta\left(\frac{\partial u}{\partial t} - v\right) = -\left(\frac{k_{\mathrm{B}}T\phi}{V_{\mathrm{m}}(1-\phi)}\right)\nabla\phi \tag{C10}$$

For small ϕ, this should reproduce normal diffusion. Using that $C_{\mathrm{m}}\approx\phi/V_{\mathrm{m}}$ is the concentration of gel monomer per fluid volume, we get:

$$\zeta\left(\frac{\partial u}{\partial t} - v\right) = -k_{\mathrm{B}}TC_{\mathrm{m}}\nabla C_{\mathrm{m}} \tag{C11}$$

For normal diffusion, the drag coefficient, ζ_{D}, is defined as the drag per particle. In our representation, ζ is the drag per total volume. The relation between these is $\zeta = \zeta_{\mathrm{D}}C_{\mathrm{m}}$, which shows that these equations reproduce pure diffusive behavior when only entropic effects are considered and we recover the Einstein relation for the diffusion coefficient, $D = k_{\mathrm{B}}T/\zeta_{\mathrm{D}}$.

Appendix D: linear approximation

The gel equations are a coupled, nonlinear set of equations. To gain insight into the dynamics that they describe, we linearize the isotropic expansion equations about an initial polymer volume fraction, ϕ_{init}, setting $\phi = \phi_{\mathrm{init}}(1-\epsilon)$, and using the rescalings $u \to Lu$, with L a relevant length scale. We use Eqs. (3), (5), and (7), and expand to first order in ϵ to obtain:

$$\begin{aligned} \varepsilon &\approx -\nabla u \\ u_t &= \left(A\nabla^2 u + B\nabla\times(\nabla\times u)\right) \end{aligned} \tag{D1}$$

where:

$$A = (1 - \phi_{\mathrm{init}})(4\tilde{\mu}/3 + \phi_{\mathrm{init}}(\partial h/\partial\phi_{\mathrm{init}})) \tag{D2}$$

and:

$$B = (1 - \phi_{\mathrm{init}})(\tilde{\mu}/3 + \phi_{\mathrm{init}}(\partial h/\partial\phi_{\mathrm{init}})) \tag{D3}$$

with:

$$\tilde{\mu} = (V_{\mathrm{m}}/k_{\mathrm{B}}T)\mu \tag{D4}$$

h is the dimensionless swelling pressure that is derived in Appendix C, and $\partial h/\partial\phi_{\mathrm{init}}$ the derivative of h with respect to ϕ evaluated at $\phi = \phi_{\mathrm{init}}$. The latter is equivalent to the equation derived by Tanaka et al. (1973) with bulk modulus:

$$K = (k_{\mathrm{B}}T/V_{\mathrm{m}})(1 - \phi_{\mathrm{init}})\phi_{\mathrm{init}}(\partial h/\partial\phi) \tag{D5}$$

This equation can now be used to calculate the rate of change in polymer volume fraction and the fluid velocity for swelling of a gel near some initial configuration ϕ_{init}. This can then be compared with the work that has already been done on spherical swelling which has neglected fluid velocity.

We begin by assuming that all variables are only functions of r, the radial coordinate, and that all vectors are only in the radial direction, $u = u(r)\hat{r}$ and $v = v(r)\hat{r}$. This allows the conservation equation to be integrated and the solvent velocity is obtained in terms of the polymer velocity:

$$v(r) = \frac{c(t)}{(1-\phi)r^2} - \frac{\phi u_t}{(1-\phi)} \tag{D6}$$

with $c(t)$ a time-dependent constant. For a finite solution at $r = 0$, $c(t) = 0$, giving $(1-\phi)v + \phi u_t = 0$, i.e. the center of mass of the gel is stationary. Thus $v > 0$ for hydrating gels; the fluid flows into the gel at a velocity equal to the ratio of gel volume to fluid volume. Using this result, the first-order polymer velocity equation is:

$$u_t \approx \left(\tilde{\mu} + \phi_{\mathrm{init}}\frac{\partial h}{\partial\phi_{\mathrm{init}}}\right)\nabla_r^2 u \tag{D7}$$

with ∇_r being the radial gradient. This gives a diffusive dynamics:

$$u_t = -D\nabla_r^2 u \tag{D8}$$

with a diffusion coefficient:

$$D = -\frac{k_{\mathrm{B}}T}{\zeta V_{\mathrm{m}}}(1 - \phi_{\mathrm{init}})\left(\tilde{\mu} + \phi_{\mathrm{init}}\frac{\partial h}{\partial\phi_{\mathrm{init}}}\right) \tag{D9}$$

[The minus sign in the diffusion constant is due to the fact that as the gel swells, the displacement increases. In Eq. (D9), $D > 0$.] If we assume a neutral gel, $\alpha = 0$, and utilize reasonable values of $\phi_0 = 0.1$, $V_{\mathrm{m}} = 10^{-22}$ cm^3, $\chi = 0.6$, $N_{\mathrm{x}} = 60$ (English et al. 1996), $\mu = 200$ dyn/cm^2, and $\zeta = 2\times10^{11}$ dyn s/cm^4 (Tanaka and Fillmore 1979), we find $D = 6.8\times10^{-7}$ cm^2/s with $\phi_{\mathrm{init}} = 0.05$ and $D = 4.7\times10^{-7}$ cm^2/s with $\phi_{\mathrm{init}} = 0.025$, which are comparable to the diffusion constants previously observed for gels with these polymer volume fractions and the ratio $D_5/D_{2.5} = 1.45$ is what is experimentally observed (Tanaka et al. 1973). Using the continuity equation (Eq. 2) and the linearized equations, we obtain the effective diffusion equation for the polymer volume fraction:

$$\varepsilon_t = D\nabla_r^2 \varepsilon \tag{D10}$$

When the gel/solvent interface is sufficiently permeable, water can flow into the gel to satisfy any imposed boundary condition on the gel. Using a zero stress boundary condition sets the polymer volume fraction at the interface to the unstressed volume fraction and the gel will relax to this unstressed state on a characteristic time scale given by $\tau \approx L^2/D$. This time decreases as the charge per monomer, α, is increased. Therefore, a polyelectrolyte gel swells faster than a neutral gel, as is observed experimentally.

To calculate the swelling radius versus time for the linear approximation of the spherically symmetric gel, we use the result derived in Tanaka and Fillmore (1979):

$$\Delta a(t) = \left(\frac{6}{\pi^2}\right)\Delta a_0 \sum n^{-2} exp\left(\frac{-Dn^2 t}{a^2}\right) \tag{D11}$$

where Δa is the change in radius of the gel, Δa_0 is the total change in radius, D is the diffusion coefficient found in Eq. (D9) and the sum is over n.

Appendix E: equations for the swelling gel

In this Appendix, we derive a dynamic equation for the polymer volume fraction, ϕ, in a Lagrangian frame of reference with respect to the initial coordinates. The coupled dynamic equations for the gel can be reduced to one equation by neglecting shear. Symmetry conditions permit this for certain geometries (e.g., spheres and slabs). For other geometries, the magnitude of the shear term is a few orders of magnitude smaller than that of the volume deformation term for a wide range of physically relevant parameters (Tanaka and Fillmore 1979). Moreover, we will see that neglecting shear greatly simplifies the analysis, yet fits the experimental data closely.

For the purposes of our calculations, it is easier to work in a reference frame fixed on the initial position of the gel, since this frame does not change in time. In this frame, the continuity equation for the polymer volume fraction does not contain convection, and, therefore:

$$\partial_t|_x \phi = -\phi \nabla_X \cdot 2u_t \tag{E1}$$

where $\partial_t|_x$ represents the partial derivative with respect to time at fixed material point x_{init}. Derivatives with respect to the initial position are given by:

$$\frac{\partial}{\partial X_i} = \left(\frac{\partial x_{init,j}}{\partial X_i}\right)\frac{\partial}{\partial x_{init,j}} \tag{E2}$$

and we can define the metric as:

$$g_{ij} = \frac{\partial X_k}{\partial x_{init,i}}\frac{\partial X_k}{\partial x_{init,j}} \tag{E3}$$

Substituting Eq. (5) into Eq. (2) and adding and subtracting the divergence of the polymer velocity, yields:

$$\nabla_X \cdot \left(\frac{1}{\zeta}(\phi - 1)2f^p + 2u_t\right) = 0 \tag{E4}$$

Plugging this into Eq. (E1) and using Eqs. (E2) and (E3) leads to a dynamic equation for ϕ:

$$\partial_t|_x \phi = -\frac{\phi^2}{\phi_{init}}\frac{\partial}{\partial x_{init,i}}\left(\frac{\phi_{init}}{\zeta\phi}(1 - \phi)f_i^p\right) \tag{E5}$$

where f_i^p is the ith component of the polymer force and it has been used that the metric determinant:

$$g^{1/2} = \phi_{init}/\phi \tag{E6}$$

For a spherically symmetric gel:

$$\left(\frac{R}{r}\right)^2\frac{\partial R}{\partial r} = \frac{\phi_{init}}{\phi} \tag{E7}$$

where R is the radial coordinate and r is the radius of the initial state.

If shear is neglected, and we assume isotropy:

$$g^{ij} = \left(\frac{\phi}{\phi_{init}}\right)^{2/d}\delta^{ij} \tag{E8}$$

where d is the dimension of space and δ^{ij} is the Kroencker delta function, then the polymer force can be written completely in terms of ϕ and $\partial\phi/\partial x_{init}$. This simplifies the dynamics by giving a single nonlinear PDE for ϕ rather than the coupled set of equations (Eqs. 2, 3, 4, 5), and greatly simplifies the problem.

For the drug delivery swelling problem, Eq. (E5) was solved numerically on a spherically symmetric volume with initial volume fraction $\phi_0 = 0.95$ everywhere, except at the boundary point where we seed the low-energy swollen state with $\phi = 0.1$. We used boundary conditions (see Eq. F1) with the drag coefficient discussed in Appendix G. The microscopic energy parameters were found from fits to the experimental data (see Appendix G). Equation (E5) was solved on the fixed initial coordinates using a variable time step method (MATLAB routine ode15s) and a forward explicit numerical scheme.

Appendix F: boundary conditions for a swelling gel

Taking the functional derivative of the free energy produces both an integral over the volume and surface terms [see, for example, Eq. (A8)]. The integrand of the volume integral gives the force per volume that acts on the gel. The integrand of the surface area integral provides the *natural boundary conditions* on the stress. In circumstances where there are no external forces acting, these boundary conditions apply. For the swelling gel, the natural boundary conditions are:

$$\sigma^{\mathrm{p}} \cdot \hat{n} \quad = \quad 0$$
$$\gamma\phi\nabla\phi \cdot \hat{n} \quad = \quad 0 \tag{F1}$$

Tokita and Tanaka (1991) found that $\zeta \propto \phi^{1.5}$ when $\phi < 1$; this is expected from Flory scaling theory since the drag coefficient scales like $1/\xi^2$, where ξ is the length correlation for the gel. Scaling theory suggests that $\xi \propto \phi^{-3/4}$. We use this dependence for the drag coefficient. We assume a volume fraction dependence on γ, and find the best fits to the data when $\gamma \propto \phi^{-1}$.

Appendix G: parameter fits from swelling experiments

Our model depends on a number of microscopic parameters that describe the material and physical properties of gels. The data of Budtova and Navard (1998) allow us to fit a number of the microscopic parameters in this model and enable us to fit the dynamic behavior of the swelling of dry gels (see Fig. 2 and Fig. 3). In fig. 2 of Budtova and Navard (1998), the swelling curves for spherical poly(0.75 sodium acrylate–0.25 acrylic acid) gels of differing radii are plotted. The bath ion concentration for this plot is $C_{\mathrm{b}} = 0$. Based on the mole fraction of the crosslinking density to that of the monomer, an estimate of the number of monomers per crosslink for these gels is $N_{\mathrm{x}} = 1600$ (Budtova and Navard 1998). If we assume that the volume of a monomer is ~0.1 nm^3 (English et al. 1996), then the only parameters left to fit are χ, α_0, ζ, and ϕ_0. ζ sets the overall time scale for the process, and is found by scaling the computer time (time step interval) to the experimental time, giving $\zeta(\phi = 1) \approx 10^{13}$ dyn s/cm^4, which is comparable to experiment (Tokita and Tanaka 1991). χ_0, α_0, and ϕ_0 were fit to provide a swelling ratio comparable to that observed in the experiments (Budtova and Navard 1998). χ_1 was set by fitting the experimental swelling data to the numerical results. We find $\chi = 0.6 + 2.3\phi^2$, $\alpha_0 = 1.0$, and $\phi_0 = 0.5$. These values are reasonable compared to what has been measured previously (English et al. 1996).

Appendix H: model equations for cell crawling

We model the dynamics of the 1-D cytoskeletal strip of gel with the following four equations:

$$\frac{\phi_{\mathrm{init}}}{\phi} = 1 + \frac{\partial u}{\partial x} \tag{H1}$$

$$\frac{\partial}{\partial x}\left(\phi\frac{\partial u}{\partial t} + (1 - \phi)v\right) = 0 \tag{H2}$$

$$\zeta\left(v - \frac{\partial u}{\partial t}\right) = -\frac{\partial p}{\partial x} \tag{H3}$$

$$\zeta_{\mathrm{ex}}\frac{\partial u}{\partial t} + \zeta\left(\frac{\partial u}{\partial t} - v\right) = \frac{\partial \sigma^{\mathrm{p}}}{\partial x} \tag{H4}$$

Here Eqs. (H1) and (H2) are 1-D conservation equations for the polymer (Eq. 3) and the gel (Eq. 2), respectively. Equation (H3) is the 1-D force balance for the liquid (Eq. 4). Finally, Eq. (H4) is the 1-D gel force balance (Eq. 5), where we have added the effective viscous drag between the cytoskeleton and the surface; ζ_{ex} is the corresponding viscous drag coefficient. The gel stress is:

$$\sigma^{\mathrm{p}}(\phi) = (k_{\mathrm{B}}T/V_{\mathrm{site}})h(\phi) \tag{H5}$$

where the stress due to changes in volume, $h(\phi)$ is given by Eq. (C8). The shear terms are absent in 1-D in both the polymer and liquid force balance equations. We solve the problem on the moving boundary domain $r(t) < x < f(t)$, where $r(t)$ and $f(t)$ are the coordinates of the rear and front of the cell, respectively. The rates of movement of the cell edges are given by the gel velocities at the edges, plus the rate of polymerization at the front and depolymerization at the rear, respectively. Thus the boundary conditions are:

$$\frac{\mathrm{d}r}{\mathrm{d}t} = V_{\mathrm{d}} + \frac{\partial u}{\partial t}|_{x=r(t)}, \quad \frac{\mathrm{d}f}{\mathrm{d}t} = V_{\mathrm{p}}(r,f) + \frac{\partial u}{\partial t}|_{x=f(t)}, V_{\mathrm{p}}(r,f)$$
$$= \frac{V_{\mathrm{p}}^0}{f - r - l_1} \tag{H6}$$

Here V_{d} is the constant depolymerization rate. The polymerization (protrusion) rate at the front is the decreasing function of the cell length, $l(t) = f(t) - r(t)$; l_1 is a model parameter.

We assume that the pH gradient regulates the external drag coefficient so that $\zeta_{\mathrm{ex}} = 3\zeta(1 + 0.8 \cdot \tanh((x - r - l_2)/l_3))$, where l_2 and l_3 are model parameters. (The internal drag coefficient, ζ, is given in Table 2.) The external drag coefficient is small and almost constant under the cell body but constant and large under the lamellipod. We also assume that the number of dimers between the adjacent crosslinks in the gel increases significantly from 25 at the front to 75 at the rear. We describe this effect quantitatively with a function similar to drag coefficient spatial behavior: $N_{\mathrm{x}} = 50 - 25 \tanh((x - r - l_2)/l_3)$. Finally, we reason that the equilibrium volume fraction of the gel scales as $\phi \propto N_{\mathrm{x}}^{1/2}$. Indeed, the equilibrium size of a long flexible filament is proportional to the square root of its contour length (Landau et al. 1980). Thus, the number of MSP dimers in unit volume scales like the number of dimers between the adjacent crosslinks divided by the equilibrium distance between these crosslinks, $N_{\mathrm{x}}/N_{\mathrm{x}}^{1/2}$. Therefore, we assume that:

$$\phi_0 = 0.005 N_{\mathrm{x}}^{1/2} \tag{H7}$$

where the coefficient is set such that the equilibrium volume fraction at the front is approximately 0.035. as is observed experimentally. For simplicity, we keep other model parameters constant; they are given in Table 2. In simulations, we used the length scale $L = 10$ µm, the time scale:

$$\zeta V_{\text{site}} L^2 / k_B T \approx 0.01 \text{ s} \tag{H8}$$

and the force scale:

$$k_B T L^2 / V_{\text{site}} \approx 100 \text{ dyn} \tag{H9}$$

We also used additional parameters: $l_1 = 5 \ \mu\text{m}$, $l_2 = 12 \ \mu\text{m}$, $l_3 = (1/15) \ \mu\text{m}$, $V_d = 0.2 \ \mu\text{m/s}$, $V_p^0 = 0.4 \mu\text{m/s}$. We non-dimensionalized the model equations using these scales.

Then, we used Eqs. (H2) and (H3) to express the fluid velocity in terms of the hydrostatic pressure gradient:

$$v = -\frac{\phi}{\varsigma} \frac{\partial p}{\partial x} \tag{H10}$$

(This equation is valid up to a constant, but this constant is almost zero due to the conditions at the leading edge, where $v = 0$, and the pressure gradient is exponentially small.) From Eqs. (H3) and (H4) we find:

$$\frac{\partial p}{\partial x} = \frac{\partial \sigma^p}{\partial x} - \varsigma_{\text{ex}} \frac{\partial u}{\partial t} \tag{H11}$$

Substituting into Eq. (H4), we obtain:

$$(\zeta_{\text{ex}}(1 - \phi) + \zeta) \frac{\partial u}{\partial t} = (1 - \phi) \frac{\partial \sigma}{\partial x} \tag{H12}$$

where:

$$\sigma = \sigma(\phi), \phi = \frac{\phi_{\text{init}}}{1 + \frac{\partial u}{\partial x}} \tag{H13}$$

We solve the equations on a uniform grid using a forward explicit integration method. At each time step, we update the gel displacement, u, using the gel stress from the previous step. Then, we use Eqs. (H10) and (H11) to find the pressure gradient and liquid velocity. Then, using Eq. (H13) we compute the new values of the gel stress using zero stress boundary conditions. Finally, we use the boundary conditions (Eq. H6) to move the cell boundaries. We start from the initial conditions of zero stress and velocities everywhere and compute until the asymptotically stable steady stress, density, and velocity distributions evolve.

References

Bottino D, Mogilner A, Roberts T, Stewart M, Oster G (2002) How nematode sperm crawl J Cell Sci 115:367–384

Bray D (2001) Cell movements: from molecules to motility, 2nd edn. Garland, New York

Budtova T, Navard P (1998) Swelling kinetics of a polyelectrolyte gel in water and salt solutions. Coexistence of swollen and collapsed phases. Macromolecules 31:8845–8850

Burge RE, Fowler AG, Reaveley DA (1977) Structure of the peptidogylcan of bacterial cell walls. I. J Mol Biol 117:927–953

Cahn JW, Hilliard JE (1958) Free energy of a nonuniform system. I. Interfacial free energy. J Chem Phys 28:258–267

Cornejo-Bravo J, Arias-Sanchez V, Alvarez-Anguiano A, Siegel R (1995) Kinetics of drug release from hydrophobic polybasic gels: effect of buffer acidity. J Controlled Release 33:223–229

Durning CJ, Morman KN Jr (1993) Nonlinear swelling of polymer gels. J Chem Phys 98:4275–4293

Elliott G, Hodson S (1998) Cornea, and the swelling of polyelectrolyte gels of biological interest. Rep Prog Phys 61:1325–1365

English AE, Mafe S, Manzanares JA, Xiahong Y, Grosberg AY, Tanaka T (1996) Equilibrium swelling properties of poly-ampholytic hydrogels. J Chem Phys 104:8713–8720

Flory P (1953) Principles of polymer chemistry. Cornell University Press, Ithaca, NY

Gu WY, Lai WM, Mow VC (1998) A mixture theory for charged-hydrated soft tissues containing multi-electrolytes: passive transport and swelling behaviors. Trans ASME J Biomech Eng 120:169–180

Happel J, Brenner H (l986) Low Reynolds number hydrodynamics, vol 1. Nijhoff, The Hague

He X, Dembo M (1997) On the mechanics of the first cleavage division of the sea urchin egg. Exp Cell Res 233:252–273

Katchalsky A, Michaeli I (1955) Polyelectrolyte gels in salt solutions. J Polym Sci 15:69–86

Lai WM, Hou JS, Mow VC (1991) A triphasic theory for the swelling and deformation behaviors of articular cartilage. J Biomech Eng 113:245–258

Landau LD, Lifshits EM, Pitaevskii LP (1980) Statistical physics, 3rd edn. Pergamon Press, Oxford

Lanir Y (1996) Plausibility of structural constitutive equations for swelling tissues-implications of the C-N and S-E conditions. Trans ASME J Biomech Eng 118:10–16

Maskawa J, Takeuchi T, Maki K, Tsujii K, Tanaka T (1999) Theory and numerical calculation of pattern formation in shrinking gels. J Chem Phys 110:10993–10999

Mogilner A, Oster G (1996) Cell motility driven by actin polymerization. Biophys J 71:3030–3045

Oliver T, Dembo M, Jacobson K (1995) Traction forces in loco-moting cells. Cell Motil Cytoskel 31:225–240

Onuki A (1989) Theory of pattern formation in gels: surface folding in highly compressible elastic bodies. Phys Rev A 39:5932–5948

Overbeek JTG (1956) The Donnan equilibrium. Prog Biophys Biophys Chem 6:58–84

Roberts T, Stewart M (2000) Acting like actin: the dynamics of the nematode major sperm protein (MSP) cytoskeleton indicate a push-pull mechanism for amoeboid cell motility. J Cell Biol 149:7–12

Sekimoto K, Suematsu N, Kawasaki K (1989) Spongelike domain structure in a two-dimensional model gel undergoing volume-phase transition. Phys Rev A 39:4912–4914

Siegel R, Falamarzian M, Firestone B, Moxley B (1988) pH-controlled release from hydrophobic/polyelectrolyte copolymer hydrogels. J Controlled Release 8:179–182

Tanaka H (1997) Viscoelastic model of phase separation. Phys Rev E 56:4451–4462

Tanaka T, Fillmore D (1979) Kinetics of swelling of gels. J Chem Phys 70:1214–1218

Tanaka T, Hocker L, Benedek G (1973) Spectrum of light scattered from a viscoelastic gel. J Chem Phys 59:5151–5159

Tokita M, Tanaka T (1991) Friction coefficient of polymer networks of gels. J Chem Phys 95:4613–4619

Tomari T, Doi M (1995) Hysteresis and incubation in the dynamics of volume transition of spherical gels. Macromolecules 28:8334–8343

Tzafriri A (2000) Mathematical modeling of diffusion-mediated release from bulk degrading matrices. J Controlled Release 63:69–79

Tzafriri A, Bercovier M, Parnas H (2002) Reaction diffusion model of the enzymatic erosion of Insoluble fibrillar matrices. Biophys J 83:776–793

Wang C, Li Y, Hu Z (1997) Swelling kinetics of polymer gels. Macromolecules 30:4727–4732

Yamaue T, Taniguchi T, Doi M (2000) Shrinking process of gels by stress-diffusion coupled dynamics. Prog Theor Phys Supp 138:416–417